
FOR THE RECORD

The three-dimensional structure of the ternary complex of *Corynebacterium glutamicum* diaminopimelate dehydrogenase-NADPH-L-2-amino-6-methylene-pimelate

MAURIZIO CIRILLI,¹ GIOVANNA SCAPIN,³ ANDREW SUTHERLAND,² JOHN C. VEDERAS,²
AND JOHN S. BLANCHARD³

¹Instituto Strutturista Chimica—CNR, Via Salaria, Rome, Italy

²Department of Chemistry, University of Alberta, Edmonton, Alberta T6G 2G2, Canada

³Department of Biochemistry, Albert Einstein College of Medicine, 1300 Morris Park Avenue, Bronx, New York 10461

(RECEIVED May 17, 2000; FINAL REVISION July 24, 2000; ACCEPTED July 24, 2000)

Abstract: The three-dimensional (3D) structure of *Corynebacterium glutamicum* diaminopimelate D-dehydrogenase in a ternary complex with NADPH and L-2-amino-6-methylene-pimelate has been solved and refined to a resolution of 2.1 Å. L-2-Amino-6-methylene-pimelate was recently synthesized and shown to be a potent competitive inhibitor (5 μM) vs. *meso*-diaminopimelate of the *Bacillus sphaericus* dehydrogenase (Sutherland et al., 1999). Diaminopimelate dehydrogenase catalyzes the reversible NADP⁺-dependent oxidation of the D-amino acid stereocenter of *meso*-diaminopimelate, and is the only enzyme known to catalyze the oxidative deamination of a D-amino acid. The enzyme is involved in the biosynthesis of *meso*-diaminopimelate and L-lysine from L-aspartate, a biosynthetic pathway of considerable interest because it is essential for growth of certain bacteria. The dehydrogenase is found in a limited number of species of bacteria, as opposed to the alternative succinylase and acetylase pathways that are widely distributed in bacteria and plants. The structure of the ternary complex reported here provides a structural rationale for the nature and potency of the inhibition exhibited by the unsaturated L-2-amino-6-methylene-pimelate against the dehydrogenase. In particular, we compare the present structure with other structures containing either bound substrate, *meso*-diaminopimelate, or a conformationally restricted isoxazoline inhibitor. We have identified a significant interaction between the α-L-amino group of the unsaturated inhibitor and the indole ring of Trp144 that may account for the tight binding of this inhibitor.

The biosynthesis of *meso*-diaminopimelate, and its subsequent decarboxylation to form L-lysine, is restricted to bacteria, plants, and fungi. Mammals lack the capacity to synthesize L-lysine and must obtain this amino acid in their diet. Bacteria and plants biosynthe-

size L-lysine via the *meso*-diaminopimelate pathway, while fungi use the alternative amino adipate pathway. The bacterial biosynthetic pathway has been thoroughly explored due to the potential for exploitation of inhibitors of enzymes in the pathway as antibacterial agents and herbicides (Cox, 1996; Scapin & Blanchard, 1997). Three pathways exist in bacteria for the biosynthesis of *meso*-diaminopimelate (Fig. 1): the ubiquitous succinylase pathway, the more restricted acetylase pathway, and the dehydrogenase pathway, identified to date only in *Corynebacteria*, and several *Bacillus* and *Brevibacterium* species (Misono et al., 1986; Ishino et al., 1987). In *Corynebacterium glutamicum*, both the succinylase and dehydrogenase pathways have been shown to be present and operate simultaneously (Schrumphf et al., 1991), with 30% of the L-lysine produced via the dehydrogenase pathway and with the remainder produced via the succinylase pathway (Sonntag et al., 1993).

The NADPH-dependent diaminopimelate dehydrogenase (DapDH; EC 1.4.1.16) catalyzes the reductive amination of L-2-amino-6-oxo-pimelate, the acyclic form of L-tetrahydrodipicolinate, to generate the *meso* compound, D,L-diaminopimelate. This chemistry is well represented in biochemistry and is catalyzed by the family of amino acid dehydrogenases that include L-glutamate, L-leucinem, and L-phenylalanine dehydrogenases. The three-dimensional (3D) structures of each of these enzymes has been determined (Stillman et al., 1993; Baker et al., 1995; Vanhooke et al., 1999), as have the 3D structures of the *C. glutamicum* diaminopimelate dehydrogenase in complex with NADP⁺ (Scapin et al., 1996), its substrate, D,L-diaminopimelate, and an isoxazoline inhibitor (Scapin et al., 1998). The noncompetitive nature of the inhibition by the isoxazoline inhibitor was shown to be due to the unexpected binding of the inhibitor in an orientation opposite to that expected, i.e., with the L-amino acid center not in the distal pocket but rather adjacent to the bound nucleotide. The synthesis of L-2-amino-6-methylene-diaminopimelate, and the report of its potent, competitive inhibition of the *Bacillus sphaericus* diaminopimelate dehydrogenase (Sutherland et al., 1999) led us to attempt to crystallize the ternary dehydrogenase-nucleotide-L-2-amino-6-methylene-diaminopimelate complex to assess the mode of binding and rationalize the very strong binding of this inhibitor relative to the substrate.

Reprint requests to: John S. Blanchard, Albert Einstein College of Medicine, Department of Biochemistry, Yeshiva University, 1300 Morris Park Avenue, Bronx, New York 10461; e-mail: blanchar@aecom.yu.edu.

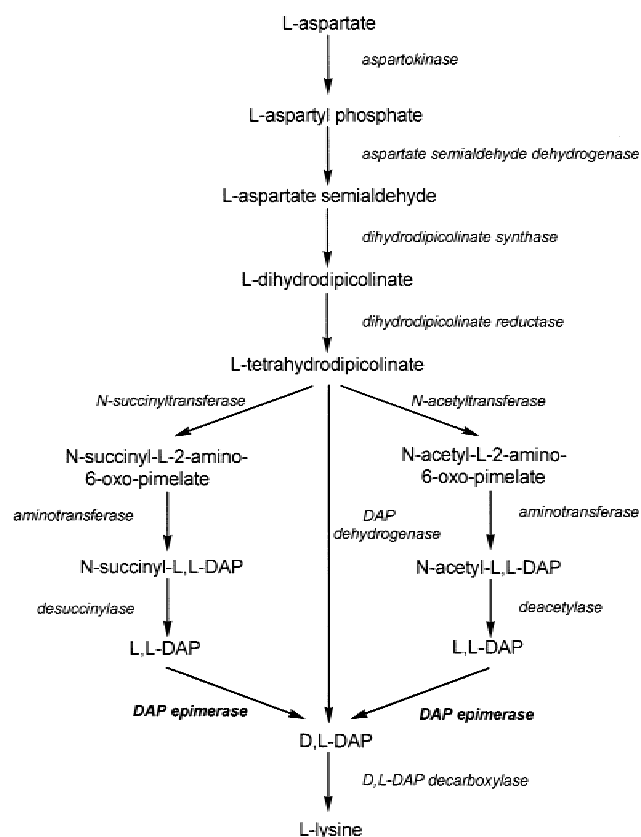


Fig. 1. Bacterial pathways for the biosynthesis of *meso*-DAP and L-lysine.

Crystals of the ternary complex were obtained in the same monoclinic space group previously obtained (Scapin et al., 1998), conforming to the “closed” conformation. These crystals diffracted to >2.1 Å. The structure of the ternary complex was solved by molecular replacement techniques. A ribbon depiction of one of the 320 residue monomers of the dimeric enzyme is shown in Figure 2A. Each monomer is composed of two domains: an amino-terminal nucleotide-binding domain (shown in the upper left-hand corner) and the carboxy-terminal domain involved in both dimerization and substrate/inhibitor binding. In the figure, we have included the bound L-2-amino-6-methylene-pimelate molecule to show that it binds at the interface of the two domains. The inhibitor could be easily and unambiguously placed within electron density that was apparent at the domain interface (Fig. 2B). As modeled, the inhibitor was bound in the active site in the manner predicted: the L-amino acid center was positioned at the distal L-specific amino acid binding pocket, while the 6-methylene group was positioned to mimic the intermediate imine, whose reduction by hydride transfer from NADPH would result in the formation of *meso*-DAP.

An intriguing feature of the present structure is the interactions that are observed between the unsaturated inhibitor and enzyme residues in the active site. In the binary enzyme-diaminopimelate complex, three hydrogen bonding interactions are observed between the α -carboxylate of the L-amino acid center (Arg195, Thr169, and His244), but no significant hydrogen bonding interactions are observed between the α -amino group of the L-amino acid center and the enzyme (Fig. 3A). Numerous interactions are observed between both the α -carboxylate and α -amino group of the D-amino acid center, which is positioned to both allow for, and assist, efficient hy-

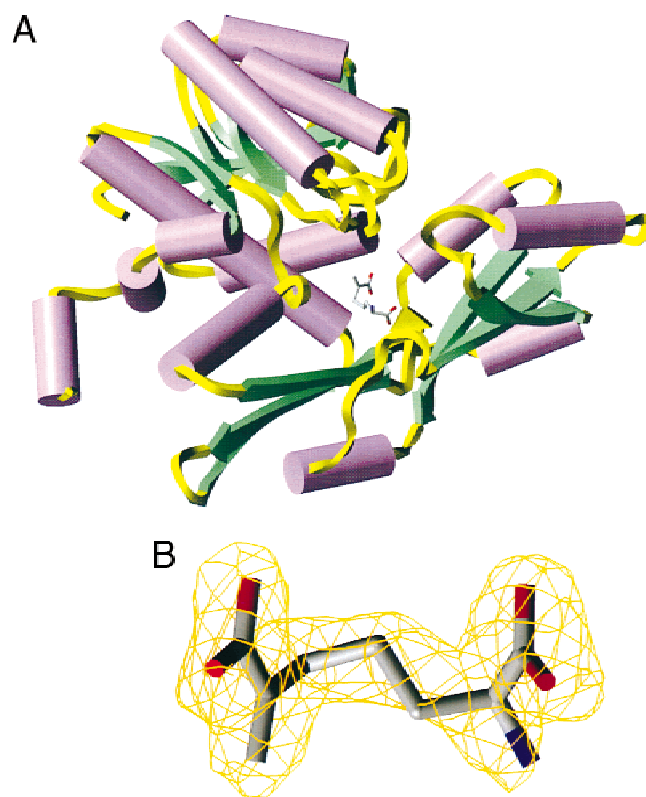


Fig. 2. **A:** Ribbon representation of a monomer of the *C. glutamicum* diaminopimelate dehydrogenase-NADPH-L-2-amino-6-methylene-pimelate complex. Helices are denoted by tubes (magenta) and β -strands as flattened arrows (green). Bound NADPH is not shown for clarity; bound L-2-amino-6-methylene-pimelate is shown at the domain interface and is colored according to atom type (C, grey; O, red; N, blue). **B:** Electron density corresponding to bound inhibitor (yellow) and final refined model of L-2-amino-6-methylene-pimelate.

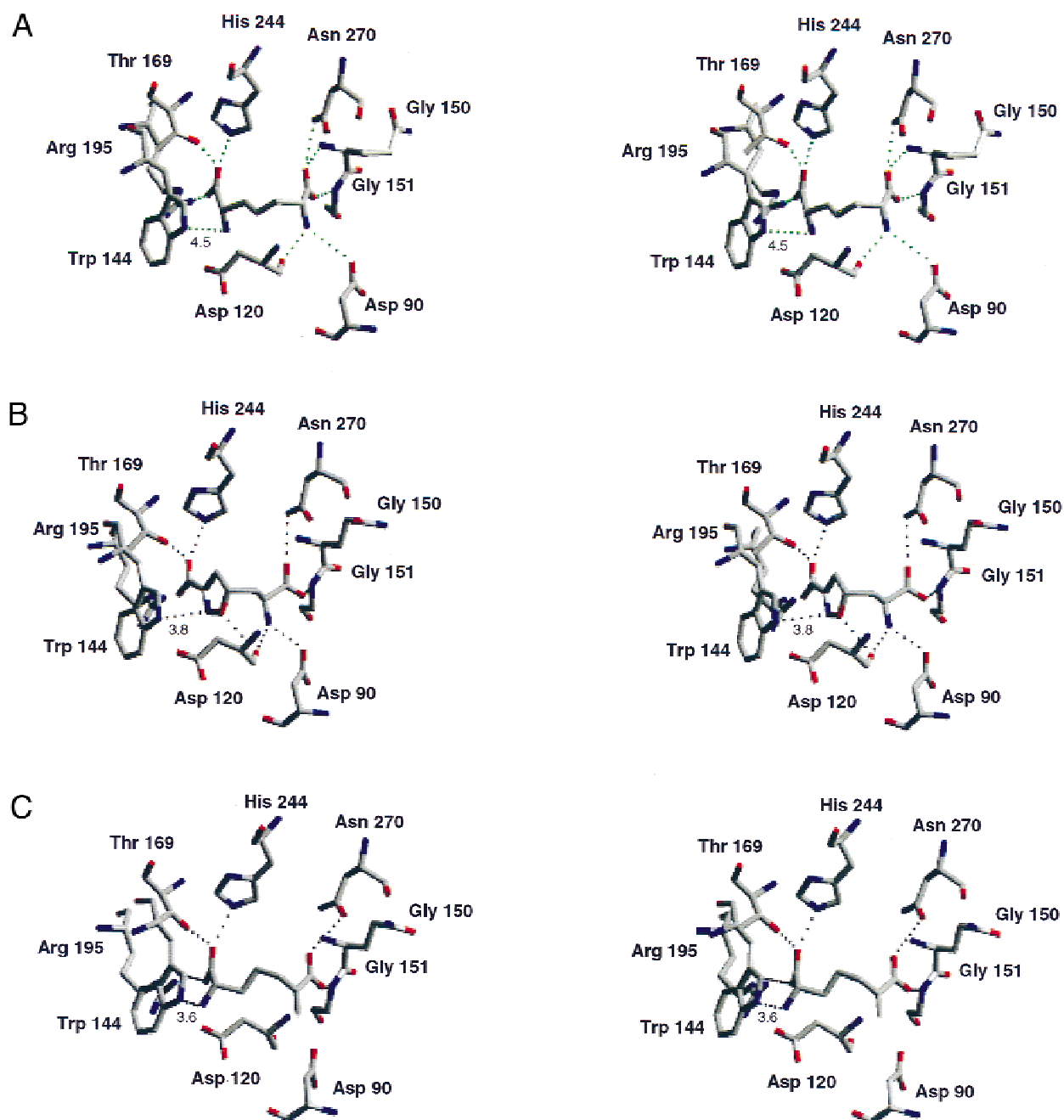


Fig. 3. Close-up view of substrate/inhibitor binding site of *C. glutamicum* diaminopimelate dehydrogenase with all residues colored according to atom type (C, grey; O, red; N, blue). **A:** *meso*-DAP bound at the active site. **B:** (2*S*,5*S*)-2-amino-3-(3-carboxy-2-isoxazolin-5-yl)-propanoic acid bound at the active site. **C:** L-2-amino-6-methylene-pimelate bound at the active site.

dride transfer to NADP^+ . In the isoxazoline inhibitor complex, the L-amino acid center is positioned where the D-center of DAP is positioned, and with the isoxazoline ring positioned such that the distal carboxylate makes hydrogen bonding interactions similar to that observed in the DAP complex (Fig. 3B). Although of opposite stereochemistry, the L-amino acid center of the isoxazoline inhibitor can make hydrogen bonds between the α -amino group of the inhibitor and the carbonyl oxygen of Asp120 and the side-chain carboxyl of Asp90. Similarly, the α -carboxylate of the L-amino acid

center makes hydrogen bonding interactions with the amido nitrogen of Asn270 and the backbone amide nitrogen of Gly151.

In the structure of the ternary enzyme-NADPH-unsaturated inhibitor, the interactions observed above are both highly conserved, and apparently maximized. Thus, while the replacement of the α -amino group of the D-stereocenter with the unsaturated methylene group results in the loss of hydrogen bonding interactions with Asp90 and Asp120, the interactions between the carboxylate of the inhibitor and both Asn270 and Gly151 are enhanced (Fig. 3C).

At the distal pocket, the interaction of the L- α -amino acid center of the inhibitor is similarly maximized, with three <2.8 Å hydrogen bonds between enzyme side chains (Arg195, Thr169, and His244) and the α -carboxylate. However, as opposed to the weak interactions between the indole nitrogen of Trp144 and either the α -amino group of the L-stereocenter of D,L-DAP, or the ring nitrogen of the isoxazoline inhibitor, the α -amino group of the unsaturated inhibitor makes a reasonable, 3.6 Å, end-on interaction with the aromatic indole ring, centered at the midpoint of the C2–C7 bond. Such aromatic rings acting as hydrogen bond acceptors for protonated amines have been observed and described in other enzyme systems previously (Burley & Petsko, 1986), and one study has estimated the strength of such a hydrogen bond as 3 kcal/mol (Levitt & Perutz, 1988). It is possible that absent interactions between the enzyme and inhibitor at the proximal amino acid binding site, due to the presence of the 6-methylene group, the unsaturated inhibitor is free to move into close contact with the indole ring of Trp144 and make the end-on aromatic-amine hydrogen bond. This structural information provides a rationale for the strong and competitive nature of the inhibition exerted by L-2-amino-6-methylene-pimelate.

Experimental: The *ddh*-encoded *C. glutamicum* diaminopimelate dehydrogenase was expressed and purified from *Escherichia coli* BL21(DE3) as described previously (Scapin et al., 1998). Crystals of the ternary dehydrogenase-NADPH-L-2-amino-6-methylene-pimelate were obtained using the vapor diffusion (hanging drop) technique in which the reservoir solution was 14% PEG8000; containing 200 mM magnesium acetate and 100 mM sodium cacodylate, pH 6.8. Crystals grew at room temperature from 4 μ L drops containing the protein (24 mg/mL in 20 mM Hepes, pH 7.5 containing 5 mM NADPH and 20 mM-L-2-amino-6-methylene-pimelate) diluted 1:1 with reservoir solution. Monoclinic crystals belonging to the space group P2₁ reached their maximum dimensions of 0.3 × 0.4 × 0.5 mm after one week. The unit cell dimensions were $a = 75.6$ Å, $b = 65.6$ Å, $c = 84.3$ Å, and $\beta = 106.5^\circ$. These crystals contained two molecules in the asymmetric unit and diffracted to a nominal maximum resolution of 2.1 Å. Diffraction data were collected at 16 °C on a Siemens multiwire area detector. Data collection and refinement statistics are shown in Table 1. The structure was solved by molecular replacement using the coordinates of the enzyme alone in the diaminopimelate dehydrogenase-NADP⁺-isoxazoline ternary complex as a starting model. Because the crystals of the two ternary complexes are isomorphous, the molecular replacement solution was straightforward. All refinement steps were carried out using the X-PLOR package (Brünger, 1992) and using all reflections observed. The refinement started with 50 cycles of rigid body minimization using data between 8.0 and 4.0 Å. Alternate cycles of simulated annealing-torsional refinement and manual rebuilding of the model were then performed. Even in the early stages of refinement, zones of residual electron density in the $(F_o - F_c)\phi_c$ map were localized in the nucleotide and substrate/inhibitor binding site. NADPH and L-2-amino-6-methylene-pimelate could be easily fitted into the electron density, and the nucleotide and inhibitor molecule were included in the model in all subsequent refinement steps. Finally, a number of water molecules were included in the model. The final model exhibits an *R*-factor of 0.178 ($R_{free} = 0.206$) with excellent geometry and RMS deviations from ideal values. The final model includes 4,998 protein atoms, 96 cofactor atoms, 13 inhibitor atoms, and 116 water molecules.

Table 1. Data collection and refinement statistics

Maximum resolution	2.1 Å
No. of observations	111,792
No. of unique reflections	39,441
Redundancy	2.8
Completeness (all shells)	87.0%
Completeness (last shell)	67.0%
<i>R</i> -merge	7.65%
Final <i>R</i> -factor	0.178
Final <i>R</i> -free	0.206
RMS deviations	
Bond lengths	0.007 Å
Bond angles	1.40°
Dihedrals	26.4°
Improvers	1.33°
Average <i>B</i> -factors (and standard deviations)	
Protein	26.9 (10.9) Å ²
NADPH	25.9 (4.4) Å ²
Inhibitor	19.7 (4.4) Å ²
Waters	32.8 (9.2) Å ²

Acknowledgments: This work was supported by NIH grant AI33696, the Natural Sciences and Engineering Research Council (NSERC) of Canada, and the Alberta Heritage Foundation for Medical Research.

References

- Baker PJ, Turnbull AP, Sedelnikova SE, Stillman TJ, Rice DW. 1995. A role for quaternary structure in the substrate specificity of leucine dehydrogenase. *Structure* 3:693–705.
- Brünger AT. 1992. *X-PLOR version 3.1 manual: A system for crystallography and NMR*. New Haven, CT: Yale University.
- Burley SK, Petsko GA. 1986. Amino-aromatic interactions in proteins. *FEBS Lett* 203:139–143.
- Cox RJ. 1996. The DAP pathway to lysine as a target for antimicrobial agents. *Nat Prod Rep* 13:29–43.
- Ishino S, Mizukami T, Yamaguchi K, Katsumata R, Araki K. 1987. Nucleotide sequence of the *meso*-diaminopimelate D-dehydrogenase gene from *Corynebacterium glutamicum*. *Nucl Acid Res* 15:3917.
- Levitt M, Perutz MF. 1988. Aromatic rings as hydrogen bond acceptors. *J Mol Biol* 201:751–754.
- Misono H, Ogaswara M, Nagasaki S. 1986. Properties of *meso*- α , ϵ -diaminopimelate D-dehydrogenase from *Bacillus sphaericus*. *Agric Biol Chem* 50:2729–2734.
- Scapin GS, Blanchard JS. 1997. Enzymology of bacterial lysine biosynthesis. *Adv Enzymol* 72A:279–324.
- Scapin GS, Cirilli M, Reddy SG, Gao Y, Vederas JC, Blanchard JS. 1998. Substrate and inhibitor binding sites in *Corynebacterium glutamicum* diaminopimelate dehydrogenase. *Biochemistry* 37:3278–3285.
- Scapin GS, Reddy SG, Blanchard JS. 1996. Three-dimensional structure of *meso*-diaminopimelate dehydrogenase from *Corynebacterium glutamicum*. *Biochemistry* 35:13540–13551.
- Schrumpf B, Schwarzer A, Kalinowski J, Puhler A, Eggeling L, Sahn H. 1991. Functionally split pathway for lysine synthesis in *Corynebacterium glutamicum*. *J Bacteriol* 173:4510–4516.
- Sonntag K, Eggeling L, De Graaf AA, Sahn H. 1993. Flux partitioning in the split pathway of lysine synthesis in *Corynebacterium glutamicum*: Quantitation by ¹³C- and ¹H-NMR. *Eur J Biochem* 213:1325–1331.
- Stillman TJ, Baker PJ, Britton KL, Rice DW. 1993. Conformational flexibility in glutamate dehydrogenase. Role of water in substrate recognition and catalysis. *J Mol Biol* 234:1131–1139.
- Sutherland A, Caplan JF, Vederas JC. 1999. Unsaturated α -aminopimelic acids as potent inhibitors of *meso*-diaminopimelic acid (DAP) D-dehydrogenase. *Chem Comm*:555–556.
- Vanhooke JL, Thoden JB, Brunhuber NMW, Blanchard JS, Holden HM. 1999. Phenylalanine dehydrogenase from *Rhodococcus* sp. M4: High resolution X-ray analyses of inhibitory ternary complexes reveal key features in the oxidative deamination mechanism. *Biochemistry* 38:2326–2329.